International Journal of Heat and Mass Transfer 51 (2008) 5804–5810

Contents lists available at ScienceDirect

International Journal of Heat and Mass Transfer

journal homepage: www.elsevier.com/locate/ijhmt

Heat and fluid flow in a rectangular microchannel filled with a porous medium

K. Hooman

School of Engineering, The University of Queensland, St. Lucia Campus, Brisbane 4072, Australia

ARTICLE INFO

Article history:
Received 21 February 2008
Received in revised form 16 May 2008
Available online 2 July 2008

Keywords:
MEMS
Fourier series approach
Microporous
Slip flow
Temperature jump

ABSTRACT

Fully developed forced convection in a rectangular microchannel filled with or without a porous medium is investigated analytically based on the Fourier series approach. The Brinkman flow model is applied with the slip velocity being accounted for. Invoking the temperature jump equation, the **H2** thermal boundary condition is investigated. Expressions are presented for the local and average velocity and temperature profiles, the friction factor, the slip coefficient, and the Nusselt number in terms of the key parameters.

1. Introduction

Microscale heat transfer has attracted researchers not only for a need to dissipate high heat transfer rates per unit area but also for playing a key rule in the biological systems [1]. Modeling convection through such small devices, with their size being in the order of 100 μm, is different from the macroscale counterparts in being associated with the inclusion of velocity slip, temperature jump, and other newly developed issues [2]. For example, a gaseous flow, say that of air, at such small passage does not obey the classical continuum physics where the no-slip condition is valid. Consequently, such a flow is associated with a nonzero fluid velocity at the solid walls and there exists a difference between the gas temperature and that of the wall. According to Tunc and Bayazitoglu [3], who studied microchannel heat transfer under slip flow and **H2** boundary condition, this can happen when $0.001 < Kn < 0.1$ while the flow is called slip flow.

Analysis of heat and fluid flow in various-shaped microchannels has been studied extensively in the past decades [4–10], to name a few. However, theoretical research on slip flow in porous-saturated microducts of arbitrary cross-section has not been conducted to the same extent. Analytical solutions are very useful in benchmarking numerical simulations. They also offer unique abilities when it comes to parametric studies with a large number of parameters involved and wherever numerical results cannot be experimentally verified. Thus, the question naturally arises as to whether analytical solutions for porous-saturated microchannels of cross-section other than circular tube or parallel plates are possible.

The complexity of the problem becomes clearer when one notes that only a handful of papers, see for example [11–18], can be mentioned when it comes to name analytical studies on macro-porous ducts of cross-sections other than circular tube or parallel plate channel (PPC), say rectangular shape, even when the saturating fluid is not a rarefied gas. Fresh numerical results of Haddad et al. [19] pertaining to convection in microporous PPC showed that the skin friction increases by increasing *Da*, decreasing *Kn*, and the Forchheimer number. Moreover, they reported that heat transfer increase as the modified Reynolds number and *Da* increase while it decreases as the Knudsen/Forchheimer number increases. Haddad et al. [20] also analyzed the effect of frequency of fluctuation of the driving force on basic slip flows in the presence of a porous medium for transient Couette flow, the pulsating Poiseuille flow, the Stokes second problem, and the transient natural convection flow. They concluded that the increase in frequency or *Kn* would lead to an increase in the normalized slip for all of the four problems mentioned above. On the other hand, the normalized slip was found to increase as *Da* plunges, except for Poiseuille flow where the normalized slip increased with *Da*. The temperature jump is reported to be negligible when the frequency and *Kn* are small. Local thermal non-equilibrium effects on slip flow forced convection in a microporous PPC were studied recently by Haddad et al. [21]. Recently, [22,23] dealt with slip flow in microtubes or micro-PPC saturated by a hyperporous medium.

Applying the Fourier series approach, this paper aims at finding the velocity and temperature distribution in a microporous duct of rectangular cross-section under slip flow and **H2** boundary condition which assumes a prescribed local wall heat flux (it emerges when the uniformly heated walls of a passage are thin with relatively low thermal conductivities). The results are found to be in

E-mail address: k.hooman@uq.edu.au

0017-9310/$ - see front matter © 2008 Elsevier Ltd. All rights reserved.
doi:10.1016/j.ijheatmasstransfer.2008.05.010

Nomenclature

a^*, b^*	microchannel dimensions (m)
A	cross-sectional area (m^2)
b	aspect (width to height) ratio
C	microduct inside periphery (m)
c_P	specific heat at constant pressure (J/kg K)
D	coefficient
Da	Darcy number
D_H	hydraulic diameter (m)
D_n	coefficient
f	friction factor
F	tangential momentum accommodation coefficient
F_t	thermal accommodation coefficient
k	effective thermal conductivity (W/m^2 K)
K	permeability (m^2)
Kn	Knudsen number
M	viscosity ratio
n^*	(coordinate) normal to the wall (m)
Nu	Nusselt number
P^*	pressure (Pa)
Pr	Prandtl number
q''	wall heat flux (W/m^2)
Re	Reynolds number
s	porous media shape parameter
T^*	local absolute temperature (K)
u^*	x-velocity (m/s)
$\hat{u}$	normalized velocity
U^*	average velocity (m/s)
v	dimensionless velocity
W	coefficient
x^*	longitudinal coordinate (m)
y^*, z^*	lateral coordinates (m)
y, z	$(y^*, z^*)/a^*$

Greek symbols

β	slip coefficient
δ	Kronecker delta
Γ	tangential coordinate at the microduct wall inside periphery (m)
γ	specific heat ratio
λ	molecular mean free path (m)
θ	dimensionless temperature
μ	fluid viscosity (N s/m^2)
μ_{eff}	effective viscosity (N s/m^2)
ρ	fluid density (kg/m^3)
ω	coefficient

Superscripts

+	of no-slip solution
*	dimensional

Subscripts

m	mean
s	slip
w	wall

complete agreement with those available in the literature of slip or no-slip flow in rectangular ducts filled with or without a porous insert.

2. Analysis

Fully developed forced convection in a microporous duct of rectangular cross-section is considered as shown by Fig. 1. The slip velocity can be found as

$$u_s^* = \frac{F-2}{F} Kn D_H \left.\frac{\partial u^*}{\partial n^*}\right|_{wall} \tag{1}$$

where u_s^* is the slip velocity, F is the tangential momentum accommodation coefficient, n^* denotes the coordinate which is normal to the wall, Kn is the Knudsen number ($Kn = \lambda/D_H$), D_H is the hydraulic diameter, and λ is the molecular mean free path. On the other hand, the fluid temperature at the wall, T_s^*, can be different from that of the wall, T_w^*, and this temperature jump can be found as

$$T_s^* - T_w^* = \frac{F_t-2}{F_t} D_H \frac{Kn}{Pr} \frac{2\gamma}{1+\gamma} \left.\frac{\partial T^*}{\partial n^*}\right|_{wall} \tag{2}$$

Though the local values of the slip velocity and the temperature jump change along the duct periphery, one can take an average over the duct periphery so that these averaged values (denoted by an over-bar) would be independent of the coordinate systems, e.g. with Γ being the tangential coordinate at a point on the microchannel wall inside periphery C, the average values (of slip velocity and temperature jump) are

$$\bar{u}_s^* = \int_C u_s^* d\Gamma / C$$
$$\bar{T}_s^* - \bar{T}_w^* = \frac{F_t-2}{F_t} \frac{Kn}{Pr} \frac{2\gamma}{1+\gamma} \frac{q'' D_H}{k} \tag{3a, b}$$

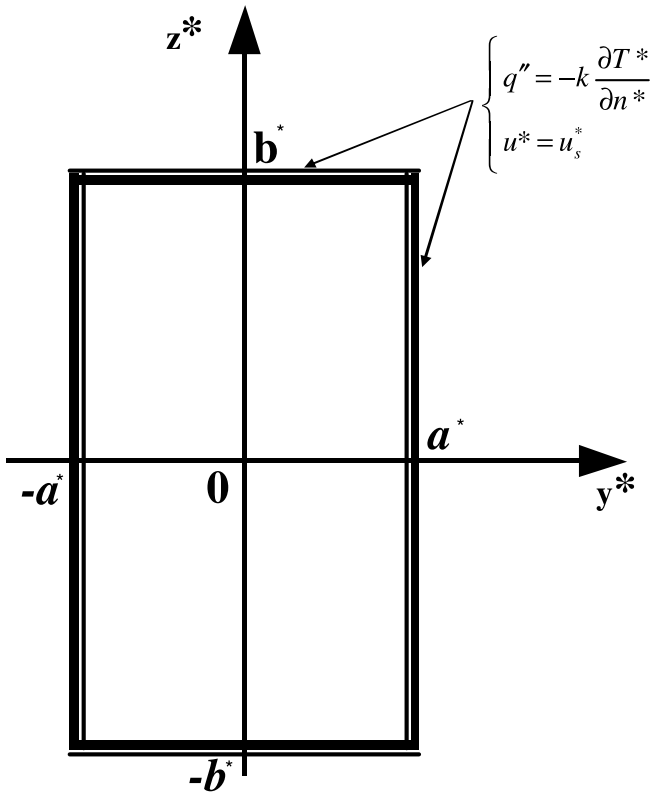

Fig. 1. A schematic of coordinates and dimensions of a microchannel cross-section.

Moreover, similar to Tunc and Bayazitoglu [3], the slip coefficient, β, is obtainable as

$$\beta = \bar{u}_s^*/U^* \tag{4}$$

where $U^* = \langle u^* \rangle$ is the average velocity with the angle brackets denoting an average taken over the microduct cross-section.

2.1. Hydrodynamic aspects of the problem

The (following) Brinkman momentum equation

$$\mu_{\text{eff}} \nabla^2 u^* - \frac{\mu u^*}{K} - \frac{\partial p^*}{\partial x^*} = 0. \tag{5}$$

should be solved subject to $u^* = \bar{u}_s^*$ at the walls. Note that the above equation reduces to the fully developed Navier–Stokes equation when $K \to \infty$ and $\mu_{\text{eff}} = \mu$.

The velocity scales with $-a^{*2}\partial p^*/\partial x^*/\mu$ so that defining the following dimensionless velocity,

$$v = -\mu(u^* - \bar{u}_s^*)/(a^{*2}\partial p^*/\partial x^*) \tag{6}$$

the momentum equation reads

$$\nabla^2 v - s^2 v + \frac{1}{M} - s^2 \bar{u}_s = 0. \tag{7}$$

that should be solved subject to $v = 0$ at the walls with M ($M = \mu_{\text{eff}}/\mu$) and s ($s = (MDa)^{-1/2}$) being the viscosity ratio and the porous medium shape parameter, respectively. Note that the Darcy number is related to the permeability as $Da = K/a^{*2}$.

The Fourier series approach assumes the following form for the velocity distribution

$$v = \sum_{n=1}^{\infty}\sum_{m=1}^{\infty} a_{mn} \cos(\beta_n y)\cos(\gamma_m z), \tag{8}$$

that satisfies the appropriate boundary conditions provided that $\beta_n = (n-1/2)\pi$ and $\gamma_m = (m\text{-}1/2)\pi/\text{b}$. the substitution of the above velocity distribution in the momentum equation leads to

$$\sum_{n=1}^{\infty}\sum_{m=1}^{\infty} (\beta_n^2 + \gamma_m^2 + s^2) a_{mn} \cos(\beta_n y)\cos(\gamma_m z) = \frac{1}{M} - s^2 \bar{u}_s \tag{9}$$

Multiplying both sides of the above equation by $\cos(\beta_n y)\cos(\gamma_m z)$ and integrating over the duct cross-section, one finds

$$a_{mn} = \frac{4}{b} \frac{(-1)^{m+n}}{(\beta_n^2 + \gamma_m^2 + s^2)\beta_n \gamma_m} \left(\frac{1}{M} - s^2 \bar{u}_s\right) \tag{10}$$

The average dimensionless slip velocity, $\bar{u}_s$, can be found, based on Eqs. (1) and (3a), as follows

$$\bar{u}_s = \frac{D}{M + Ms^2 D} \tag{11}$$

with

$$D = \frac{2-F}{F} \frac{4D_{\text{H}}}{b(1+b)} Kn \sum_{i=1}^{\infty}\sum_{j=1}^{\infty} \frac{1}{(\beta_i \gamma_j)^2} \left(\frac{\beta_i^2 + \gamma_j^2}{\beta_i^2 + \gamma_j^2 + s^2}\right) \tag{12}$$

The coefficients a_{mn} can be rearranged as

$$a_{mn} = \frac{4}{Mb} \frac{(-1)^{m+n}}{(\beta_n^2 + \gamma_m^2 + s^2)\beta_n \gamma_m} \frac{1}{1 + s^2 D} \tag{13}$$

In particular, from Eqs. (10)–(13), one finds the dimensional velocity distribution as

$$u^* = -\frac{\partial p^*}{\partial x^*} \frac{a^{*2}}{\mu_{\text{eff}}} \frac{1}{1+s^2 D} \left(\sum_{n=1}^{\infty}\sum_{m=1}^{\infty} \frac{4}{b} \frac{(-1)^{m+n}}{(\beta_n^2 + \gamma_m^2 + s^2)\beta_n \gamma_m} \times \cos(\beta_n y)\cos(\gamma_m z) + D\right) \tag{14}$$

One also obtains the average velocity as

$$U^* = -\frac{\partial p^*}{\partial x^*} \frac{a^{*2}}{\mu_{\text{eff}}} \frac{D + W}{1 + s^2 D} \tag{15a}$$

wherein

$$W = \sum_{n=1}^{\infty}\sum_{m=1}^{\infty} \frac{1}{(\beta_n^2 + \gamma_m^2 + s^2)} \left(\frac{2}{b\beta_n \gamma_m}\right)^2 \tag{15b}$$

It is now possible to find the normalized velocity as follows

$$\hat{u} = \frac{\sum_{n=1}^{\infty}\sum_{m=1}^{\infty} \frac{4}{b} \frac{(-1)^{m+n}}{(\beta_n^2 + \gamma_m^2 + s^2)\beta_n \gamma_m} \cos(\beta_n y)\cos(\gamma_m z) + D}{D + W} \tag{16}$$

It is also instructive to note that the dimensionless pressure drop, represented by *fRe*, reads

$$fRe = \left(\frac{D_{\text{H}}}{2H}\right)^2 \frac{2}{U} = 8\left(\frac{b}{1+b}\right)^2 \frac{1 + s^2 D}{D + W} \tag{17}$$

Note that the hydraulic diameter, $D_{\text{H}} = 4a^* \times b/(1+b)$, is chosen as the characteristic length in the Reynolds number, *Re*, and *f* is the pressure gradient normalized by $2\rho U^{*2}/D_{\text{H}}$.

It is an easy task to show that the slip coefficient, β, takes the following form

$$\beta = \frac{D}{D + W} \tag{18}$$

One can rearrange Eq. (17) to obtain *fRe* in terms of β as

$$fRe = (1-\beta) fRe^+ + 2\beta\left(\frac{2sb}{1+b}\right)^2 \tag{19}$$

where fRe^+ can be obtained from no-slip solutions available in the literature.

2.2. Thermal aspects of the problem

Assuming local thermal equilibrium, homogeneity, and no thermal dispersion the thermal energy equation reads

$$u^* \frac{\partial T^*}{\partial x^*} = \frac{k}{\rho c_P} \left(\frac{\partial^2 T^*}{\partial y^{*2}} + \frac{\partial^2 T^*}{\partial z^{*2}}\right). \tag{20}$$

Here T^* is the temperature, ρ the fluid density, c_P the fluid specific heat at constant pressure, and k is the effective thermal conductivity of the medium. The Nusselt number is defined as

$$Nu = \frac{q'' D_{\text{H}}}{k(T_w^* - T_m^*)}. \tag{21}$$

with the bulk temperature $T_m^* = \langle \hat{u} T^* \rangle$.

Following the application of the First Law of Thermodynamics to a thin slice of the microporous duct, the longitudinal temperature gradient, in terms of the wall heat flux, reads

$$\frac{\partial T^*}{\partial x^*} = \frac{q''}{\rho c_P a^* U^*} \frac{1+b}{b} \tag{22}$$

This, in turn, simplifies the thermal energy equation to

$$\hat{u} \frac{q''}{a^*} \frac{1+b}{b} = k\left(\frac{\partial^2 T^*}{\partial y^{*2}} + \frac{\partial^2 T^*}{\partial z^{*2}}\right). \tag{23}$$

Following the definition $\theta = kT^*/(q'' a^*)$, the dimensionless form of thermal energy equation will be

$$\hat{u} \frac{1+b}{b} = \frac{\partial^2 \theta}{\partial y^2} + \frac{\partial^2 \theta}{\partial z^2}. \tag{24}$$

that should be solved subject to the following boundary conditions

$$\left.\frac{\partial\theta}{\partial y}\right|_{y=1} = \left.\frac{\partial\theta}{\partial z}\right|_{z=b^*} = 1$$
$$\left.\frac{\partial\theta}{\partial y}\right|_{y=0} = \left.\frac{\partial\theta}{\partial z}\right|_{z=0} = 0 \qquad (25a\text{–}d)$$

Following the same steps as Haji-Sheikh [16], one has

$$\theta = \omega_{00} + \frac{W\sum_{n=0}^{\infty}\sum_{m=0}^{\infty}F_{mn}\omega_{mn}\cos(n\pi y)\cos(m\pi z/b)}{D+W} + \frac{1}{2}\left(y^2 + \frac{z^2}{b}\right) \qquad (26)$$

wherein

$$\omega_{mn} = \frac{b(1+s^2D)}{\pi^2 W}\sum_{i=1}^{\infty}\sum_{j=1}^{\infty}\frac{a_{ij}(-1)^{i+j}(i-1/2)(j-1/2)}{\left(n^2-(i-1/2)^2\right)\left(m^2-(j-1/2)^2\right)}$$
$$F_{mn} = \frac{(2-\delta_{0,n})(2-\delta_{0,m})(1-\delta_{0,m+n})(1+b^{-1})}{b\pi^2\left(n^2+(m/b)^2\right)} \qquad (27a, b)$$

The presence of the Kronecker delta, δ, indicates that the constant term ω_{00} drops following differentiating when $m = 0$ and $n = 0$; see also Haji-Sheikh [16].

Recalling Eq. (26), the average bulk and slip temperature read Finally, the Nusselt number is obtainable as

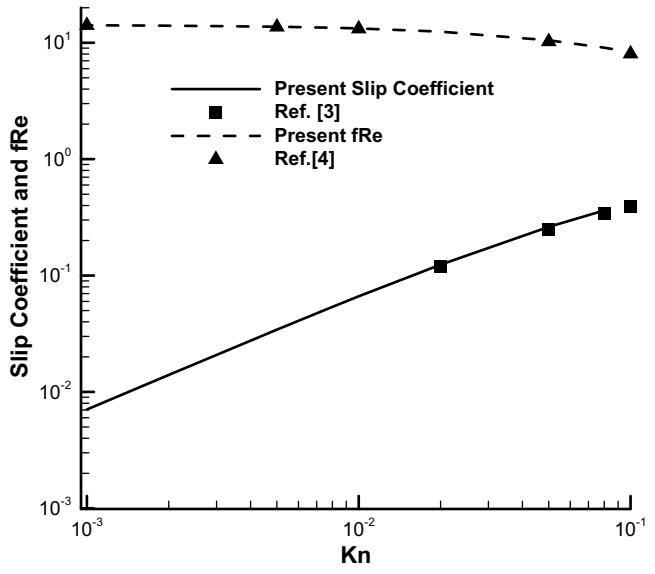

Fig. 2. Slip coefficient and *fRe* versus *Kn* compared with previous results in the literature for $s = 0$ and $b = 1$.

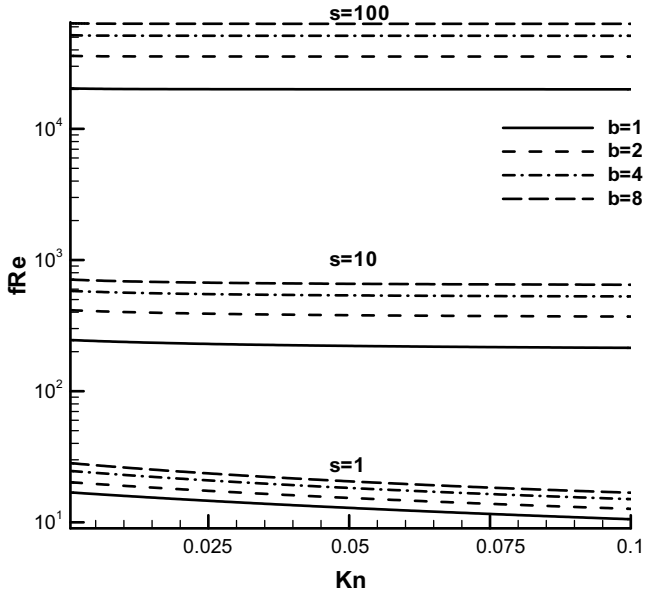

Fig. 4. *fRe* versus *Kn* for different values of *s* and *b*.

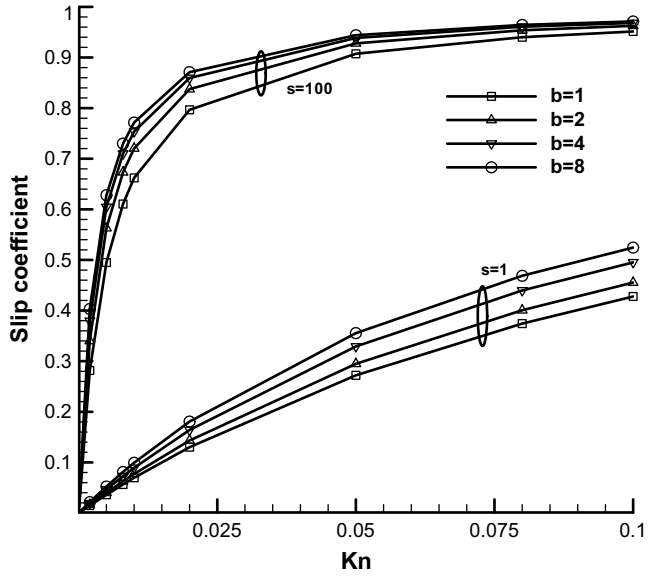

Fig. 3. Slip coefficient versus *Kn* for different values of *s* and *b*.

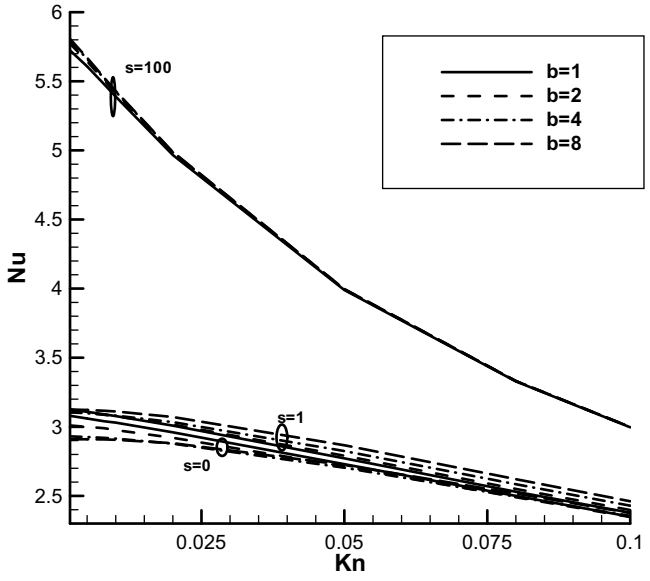

Fig. 5. The Nusselt number versus *Kn* for different values of *s* and *b*.

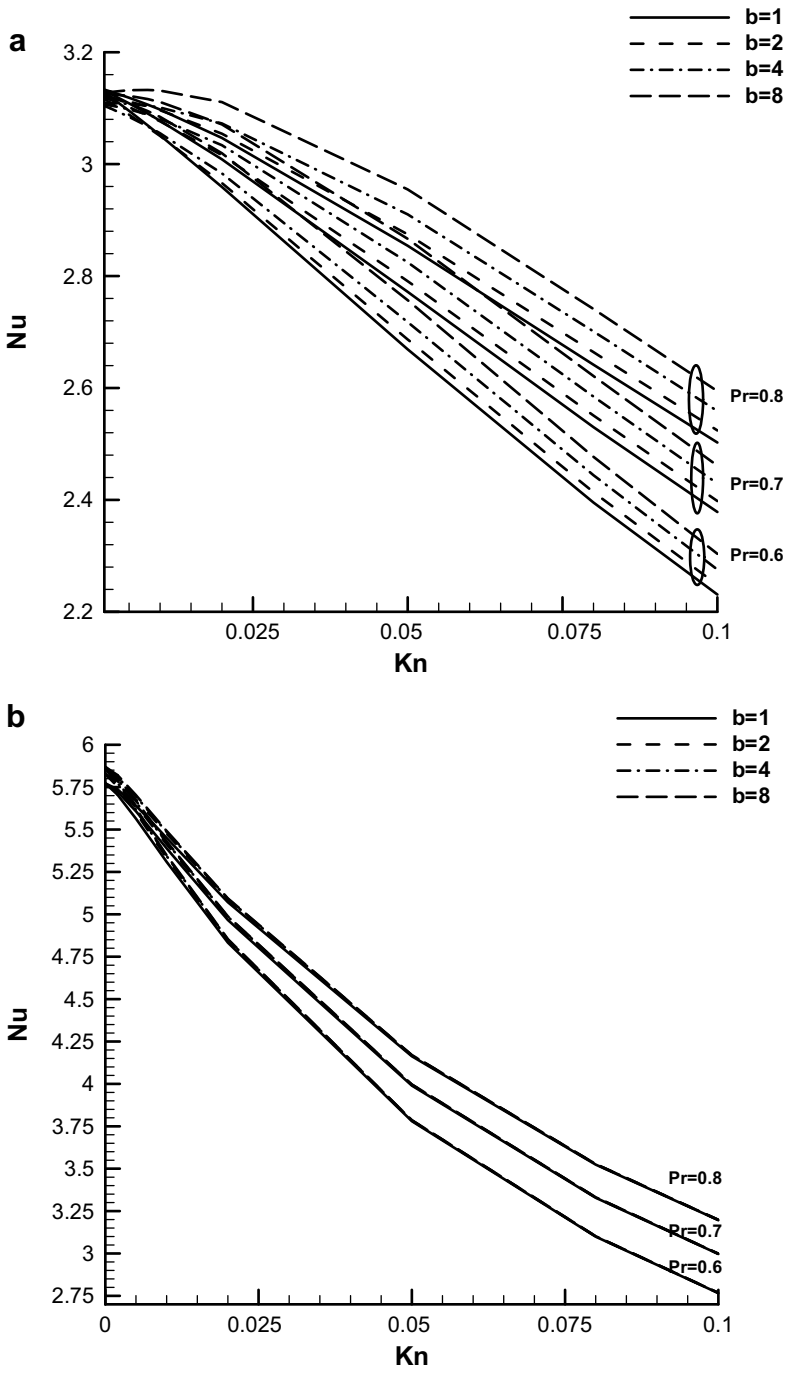

Fig. 6. Effects of *Pr* on *Nu*–*Kn* relation for different values of *b* when (a) $s = 1$, (b) $s = 100$, (c) $s = 100$ with $Kn < 0.02$.

$$\theta_m = \omega_{00} + (1+b)\frac{\beta}{6} + \frac{\frac{2M(1+s^2D)}{\pi^4}\sum_{i=1}^{\infty}\sum_{j=1}^{\infty}(-1)^{i+j}\frac{a_{ij}(\pi^2(1-4j+4j^2)-8)}{(2i-1)^3(2j-1)^3}\left[(2j-1)^2+(2i-1)^2\right] + W\sum_{n=0}^{\infty}\sum_{m=0}^{\infty}F_{mn}\omega_{mn}^2}{W+D}$$

$$\bar{\theta}_s = \omega_{00} + \frac{1+b^2+6b}{6(1+b)} + \frac{\sum_{n=0}^{\infty}\sum_{m=0}^{\infty}F_{mn}\omega_{mn}\left(\delta_{0m}(-1)^n + \delta_{0n}(-1)^m\right)}{W+D} \tag{28a, b}$$

$$Nu = \frac{D_H}{a^*(\bar{\theta}_s - \theta_m + \bar{\theta}_w - \bar{\theta}_s)} \tag{29}$$

The following dimensionless version of Eq. (3b)

$$\bar{\theta}_s - \bar{\theta}_w = \frac{F_t - 2}{F_t}\frac{Kn}{Pr}\frac{2\gamma}{1+\gamma}\frac{D_H}{a^*} \tag{30}$$

will lead to

$$Nu = \frac{1}{\frac{a^*}{D_H}(\bar{\theta}_s - \theta_m) + \frac{2-F_t}{F_t}\frac{Kn}{Pr}\frac{2\gamma}{1+\gamma}} \tag{31}$$

Note that the above expression reduces to Eq. (26) of Haji-Sheikh [16] when $Kn = 0$. Consequently, the results for Nu are in complete agreement with those of [16].

3. Results and discussion

Throughout this section we assumed $F = F_t = M = 1$ and $\gamma = 1.4$ though the closed form solutions are general enough to account for other combinations. As a sample of the results, Fig. 2 compares our fRe and β with those of [3,4] for microducts without a porous insert, i.e. when $s = 0$ and $b = 1$. The results are in complete agreement, as expected.

Fig. 3 illustrates β versus Kn for different aspect ratios with $s = 1$ and $s = 100$. As seen, in line with a previous report [24], β increases with Kn, b, and s. Observe that for $s = 100$, regardless of the aspect ratio, β asymptotically approaches its maximum value, being $\beta = 1$, as Kn increases. The increase in the slip coefficient versus Kn is expected as higher Kn values indicate higher degrees of rarefaction and, hence, deviation from continuum theory is expected as reflected in an increase in β. Moreover, as slip coefficient is a direct measure of slip velocity, which is linearly proportional to the velocity gradient at the wall, one expects that higher values of s (for which the velocity distribution is more flattened) lead to an increase in β. One can verify Eq. (16), or check the results of Hooman and Merrikh [13], for a slip and no-slip problem; respectively, to see that the velocity gradient (at the wall) increases with s.

Fig. 4 shows fRe versus Kn for $s = 1$, 10, and 100 again with different b values. Increasing s, with a fixed microduct size, means a decrease in the permeability of the porous medium so that higher values of fRe, which is linearly proportional to the pressure drop, are expected [25]. Nonetheless, with lower permeability the velocity distribution tends to be more uniform and this, in turn, leads to an increase in Nu as noted for porous marcoducts, see for example Hooman and Ranjbar-Kani [26]. Moreover, as noted by Hooman [27], with high values of s, say $s > 100$, fRe remains almost independent of Kn since for such high s values the Darcy viscous drag is predominant and fRe is almost independent of the boundary friction (Brinkman) term, see also Kaviany [28]. Note that not only O(Darcy viscous drag/Brinkman shear stress term) = O(s^2) for very high values of s but also fRe is independent of rarefaction effects, which affects the problem via the Brinkman shear stress term [27]. With higher b values, the duct cross-section is more stretched and the iso-lines for velocity are more concentrated near the walls. This means that overall velocity gradient puts on higher values as b increases. Thus fRe increases with b. This has already been observed for slip coefficient (which is, like fRe, linearly proportional to the velocity gradient at the walls).

According to Fig. 5, Nu values for $s = 1$ and $s = 0$, representing, respectively hyperporous and clear fluid case, are very close to each other while Nu for $s = 100$ puts on a value which is nearly twice that of clear fluid case for low Kn values (the Nu reduces to roughly 1.3 that of clear fluid with $Kn = 0.1$). This gives more credit to the application of the microporous heat exchangers albeit at the cost of higher pressure drop, as can be deduced from Fig. 4.

In the preceding discussion the Pr value was fixed at 0.7 so there is a need to see its effect on the Nusselt number. Fig. 6 shows Nu versus Kn for different Pr and b values with $s = 1$ and 100. One can again verify that Nu increases with both s and b. According to Fig. 6a, for each aspect ratio, Nu increases with Pr and this effect becomes more pronounced as Kn increases. Nevertheless, according to Fig. 6b, for $s = 100$ the converse is true in such a way that Pr effect on Nu is more significant when Kn is small enough. Mainly for this reason, Fig. 6c is presented to show Nu for small Kn values, being $Kn < 0.02$. For this value of s, Nu seems to be less sensitive to a change in the cross-section shape than in Pr. As a common trend in the chart on Fig. 6, one can conclude that, for nonzero values of Kn, Nu increases with Pr regardless of s or b. It should, however, be reminded that, for fully developed forced convection in macro-porous ducts, Nu is independent of Pr when $Kn = 0$.

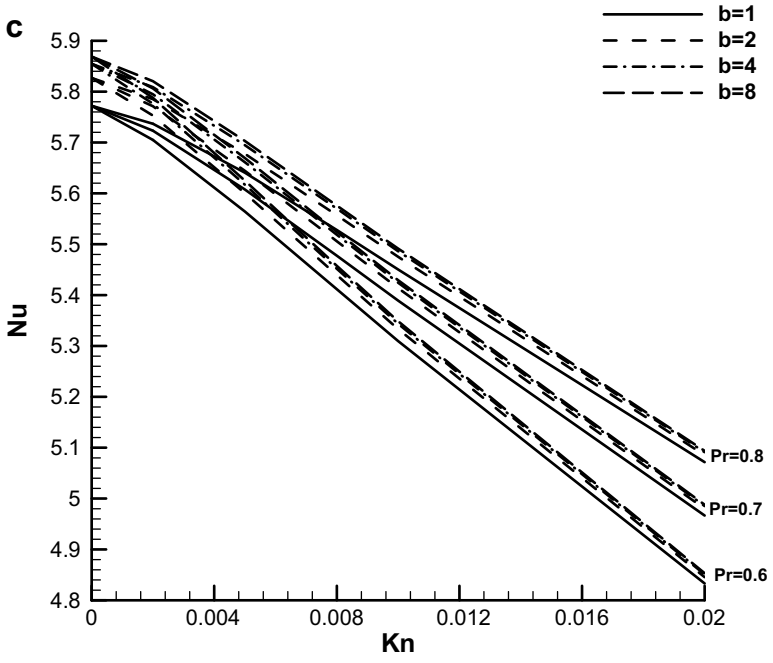

Fig. 6. (*continued*)

4. Conclusion

Applying the Brinkman flow model and **H2** thermal boundary condition, closed form solutions for fully developed velocity and temperature distribution in a microchannel of rectangular cross-section, filled with or without a porous medium, is presented with the effects of velocity slip and temperature jump being considered. Convection heat transfer and pressure drop performance of the system, reflected in *Nu* and *fRe*, respectively, on top of the velocity slip effects represented in the slip coefficient, were analyzed. Effects of the Knudsen number, Prandtl number, the porous media shape parameter, and the duct geometry on the system performance is studied. It was observed that for $s > 100$, regardless of the aspect ratio, β asymptotically approaches $\beta = 1$, as *Kn* increases while *fRe* remains almost independent of *Kn*. Increasing *s*, *b*, and *Pr*, the Nusselt number increases. The present closed form solutions can be used for benchmark checks on numerical findings for flow in micro-/macro-channels of rectangular cross-section filled with or without a porous matrix. This is a relatively important topic as reflected by the amount of numerical work addressing similar issues; see for example [28–38].

Acknowledgements

Financial support provided by The University of Queensland in terms of UQILAS, Endeavor IPRS, and School Scholarship is appreciated.

References

[1] A.A. Merrikh, J.L. Lage, The role of red cell movement on alveolar gas diffusion, Materialwissenschaft Und Werkstofftechnik 36 (10) (2005) 497–504.
[2] T.A. Ameel, X.M. Wang, R.F. Barron, R.O. Warrington, Laminar forced convection in a circular tube with constant heat flux and slip flow, Microscale Thermophys. Eng. 1 (4) (1997) 303–320.
[3] G. Tunc, Y. Bayazitoglu, Heat transfer in rectangular microchannels, Int. J. Heat Mass Transfer 45 (4) (2002) 765–773.
[4] G.L. Morini, M. Spiga, P. Tartarini, The rarefaction effect on the friction factor of gas flow in microchannels, Superlattices Microstruct. 35 (3–6) (2004) 587–599.
[5] E.M. Sparrow, A. Hajisheikh, Velocity profile and other local quantities in free-molecule tube flow, Phys. Fluids 7 (8) (1964) 1256–1261.
[6] Y. Bayazitoglu, G. Tunc, Extended slip boundary conditions for microscale heat transfer, J. Thermophys. Heat Transfer 16 (3) (2002) 472–475.
[7] X. Zhu, Q. Liao, Heat transfer for laminar slip flow in a microchannel of arbitrary cross section with complex thermal boundary conditions, Appl. Thermal Eng. 26 (11–12) (2006) 1246–1256.
[8] X. Zhu, Q. Liao, M.D. Xin, Gas flow in microchannel of arbitrary shape in slip flow regime, Nanoscale Microscale Thermophys. Eng. 10 (1) (2006) 41–54.
[9] S.P. Yu, T.A. Ameel, Slip-flow heat transfer in rectangular microchannels, Int. J. Heat Mass Transfer 44 (22) (2001) 4225–4234.
[10] K. Hooman, Entropy generation for microscale forced convection: effects of different thermal boundary conditions, velocity slip, temperature jump, viscous dissipation, and duct geometry, Int. Commun. Heat Mass Transfer 34 (8) (2007) 945–957.
[11] K. Hooman, H. Gurgenci, A.A. Merrikh, Heat transfer and entropy generation optimization of forced convection in a porous-saturated duct of rectangular cross-section, Int. J. Heat Mass Transfer 50 (2007) 2051–2059.
[12] K. Hooman, A. Haji-Sheikh, D.A. Nield, Thermally developing Brinkman–Brinkman forced convection in rectangular ducts with isothermal walls, Int. J. Heat Mass Transfer 50 (2007) 3521–3533.
[13] K. Hooman, A.A. Merrikh, Analytical solution of forced convection in a duct of rectangular cross section saturated by a porous medium, J. Heat Transfer Trans. ASME 128 (6) (2006) 596–600.
[14] A. Haji-Sheikh, D.A. Nield, K. Hooman, Heat transfer in the thermal entrance region for flow through rectangular porous passages, Int. J. Heat Mass Transfer 49 (17–18) (2006) 3004–3015.
[15] A. Haji-Sheikh, W.J. Minkowycz, E.M. Sparrow, Green's function solution of temperature field for flow in porous passages, Int. J. Heat Mass Transfer 47 (22) (2004) 4685–4695.
[16] A. Haji-Sheikh, Fully developed heat transfer to fluid flow in rectangular passages filled with porous materials, J. Heat Transfer Trans. ASME 128 (6) (2006) 550–556.
[17] A. Haji-Sheikh, K. Vafai, Analysis of flow and heat transfer in porous media imbedded inside various-shaped ducts, Int. J. Heat Mass Transfer 47 (8–9) (2004) 1889–1905.
[18] K. Hooman, H. Gurgenci, Effects of temperature-dependent viscosity variation on entropy generation, heat and fluid flow through a porous-saturated duct of rectangular cross-section, Appl. Math. Mech. (Engl. Ed.) 28 (1) (2007) 69–78.
[19] O.M. Haddad, M.A. Al-Nimr, Y. Taamneh, Hydrodynamic and thermal behavior of gas flow in microchannels filled with porous media, J. Porous Media 9 (5) (2006) 403–414.
[20] O.M. Haddad, M.A. Al-Nimr, M.M. Abuzaid, Effect of periodically oscillating driving force on basic microflows in porous media, J. Porous Media 9 (7) (2006) 695–707.
[21] O.M. Haddad, M.A. Al-Nimr, J.S. Al-Omary, Forced convection of gaseous slip-flow in porous micro-channels under local thermal non-equilibrium conditions, Transport Porous Media 67 (3) (2007) 453–471.
[22] D.A. Nield, A.V. Kuznetsov, Forced convection with slip-flow in a channel or duct occupied by a hyper-porous medium saturated by a rarefied gas, Transport Porous Media 64 (2) (2006) 161–170.
[23] A.A. Avramenko, A.V. Kuznetsov, D.A. Nield, Instability of slip flow in a channel occupied by a hyperporous medium, J. Porous Media 10 (5) (2007) 435–442.
[24] K. Hooman, A superposition approach to study slip-flow forced convection in microchannels of arbitrary cross-section, International Journal of Heat and Mass Transfer 51 (15–16) (2008) 3753–3762.
[25] K. Hooman, H. Gurgenci, Effects of viscous dissipation and boundary conditions on forced convection in a channel occupied by a saturated porous medium, Transport Porous Media 68 (3) (2007) 301–319.
[26] K. Hooman, A.A. Ranjbar-Kani, Forced convection in a fluid-saturated porous-medium tube with isoflux wall, Int. Commun. Heat Mass Transfer 30 (7) (2003) 1015–1026.
[27] K. Hooman. Slip flow forced convection in a microporous duct of rectangular cross-section, Applied Thermal Engineering, in press, doi:10.1016/j.applthermaleng.2008.05.007.
[28] M. Kaviany, Laminar-flow through a porous channel bounded by isothermal parallel plates, Int. J. Heat Mass Transfer 28 (4) (1985) 851–858.
[29] A. Amiri, K. Vafai, T.M. Kuzay, Effects of boundary-conditions on non-Darcian heat-transfer through porous-media and experimental comparisons, Numer. Heat Transfer Part A – Applications 27 (6) (1995) 651–664.
[30] R. Bradean, K. Promislow, B. Wetton, Transport phenomena in the porous cathode of a proton exchange membrane fuel cell, Numer. Heat Transfer Part A – Applications 42 (1–2) (2002) 121–138.
[31] O.M. Haddad, M.M. Abuzaid, M.A. Al-Nimr, Developing free-convection gas flow in a vertical open-ended microchannel filled with porous media, Numer. Heat Transfer Part A – Applications 48 (7) (2005) 693–710.
[32] P.X. Jiang, Z.P. Ren, B.X. Wang, Numerical simulation of forced convection heat transfer in porous plate channels using thermal equilibrium and nonthermal equilibrium models, Numer. Heat Transfer Part A – Applications 35 (1) (1999) 99–113.
[33] S.Y. Kim, J.M. Koo, A.V. Kuznetsov, Effect of anisotropy in permeability and effective thermal conductivity on thermal performance of an aluminum foam heat sink, Numer. Heat Transfer Part A – Applications 40 (1) (2001) 21–36.
[34] A.V. Kuznetsov, L. Cheng, M. Xiong, Effects of thermal dispersion and turbulence in forced convection in a composite parallel-plate channel: Investigation of constant wall heat flux and constant wall temperature cases, Numer. Heat Transfer Part A – Applications 42 (4) (2002) 365–383.
[35] A.V. Kuznetsov, D.A. Nield, Effects of heterogeneity in forced convection in a porous medium: Triple layer or conjugate problem, Numer. Heat Transfer Part A – Applications 40 (4) (2001) 363–385.
[36] M.E. Taskin, A.G. Dixon, E.H. Stitt, CFD study of fluid flow and heat transfer in a fixed bed of cylinders, Numer. Heat Transfer Part A – Applications 52 (3) (2007) 203–218.
[37] J.L. Yuan, M. Rokni, B. Sunden, A numerical investigation of gas flow and heat transfer in proton exchange membrane fuel cells, Numer. Heat Transfer Part A – Applications 44 (3) (2003) 255–280.
[38] N. Yucel, R.T. Guven, Forced-convection cooling enhancement of heated elements in a parallel-plate channels using porous inserts, Numer. Heat Transfer Part A – Applications 51 (3) (2007) 293–312.